

EXPERIMENTAL AND NUMERICAL STUDY OF MARANGONI CONVECTION IN A  
SANDWICHED DROPLET

by

AJINKYA SHRIKRISHNA SHETYE

Presented to the Faculty of the Graduate School of  
The University of Texas at Arlington in Partial Fulfillment  
of the Requirements  
for the Degree of

MASTER OF SCIENCE IN MECHANICAL ENGINEERING

THE UNIVERSITY OF TEXAS AT ARLINGTON

MAY 2016

Copyright © by Ajinkya Shrikrishna Shetye 2016

All Rights Reserved



## Acknowledgements

I would like to dedicate this thesis to my mother whose love and sacrifices made me achieve this. I thank my father for setting a good example of a person who never gives up. I am indebted to my brother and sister-in-law who had faith in me and supported me in everything. Master program would not have been possible without them.

I am grateful to my supervisor Dr. Hyejin Moon for giving me an opportunity to perform research under her guidance. She is one of my reasons for coming to UTA. It is rightly being said that “*Give a man a fish and you feed him for a day; teach a man to fish and you feed him for a lifetime*” I believe she preaches the latter part of the quote which has transformed me into an independent thinker. I cannot thank her enough for making my master program worthwhile.

Special thanks go to my labmates, Mun Mun Nahar and Ali Farzbod, for guiding me whenever I struggled in my research and encouraged me to work hard. I feel fortunate to work with them. I thank Arvind Venkatesan and Shubhodeep Paul for helping me in many ways, both in research and in academics. It is an honor to be a part of “*Integrated Micro and Nanofluidics Laboratory*”. I thank to all my other labmates for creating a great environment in the lab. Research would not have been fun without them. I would like to thank my friend Sanmitra Saudatti for helping me with editing. I give a big thank to my roommates, Rohit Kulkarni, Yogesh Patekari and Aniket Kadam, for their encouragement and support.

April 12, 2016

## Abstract

### EXPERIMENTAL AND NUMERICAL STUDY OF MARANGONI CONVECTION IN A SANDWICHED DROPLET

Ajinkya Shrikrishna Shetye, MS

The University of Texas at Arlington, 2016

Supervising Professor: Hyejin Moon

This research studies velocity fields resulted from the marangoni effect in a microscale droplet sandwiched in parallel plates. Surface tension becomes the dominant driving force as opposed to body forces as we move from the macroscale to microscale. Surface tension gradient is required to generate marangoni convection. This could be produced by a temperature gradient along the meniscus of the drop. To study this interfacial phenomenon, indium tin oxide micro thin film heater is utilized to create the necessary temperature gradient. Pure marangoni effect is studied by suppressing the evaporation effect on fluid flow by using an ionic liquid (molten salt) as the working fluid. Flow patterns have been visualized using nylon seeding particles under a polarized light microscope. The temperature distribution and velocity of the particles have been obtained using liquid crystal thermography (LCT) and micro particle image velocimetry ( $\mu$ PIV). The experimental data was validated by finite element analysis in COMSOL Multiphysics software. With recent advancements in the study of thermocapillary effect, microfluidic applications utilizing marangoni convection are gaining momentum. Applications include thermocapillary pumps, micromixers, actuators and sensors.

## Table of Contents

Acknowledgements .....	iii
Abstract .....	iv
List of Illustration.....	vii
List of Tables.....	ix
Chapter 1 INTRODUCTION.....	1
1.1 Motivation.....	1
1.2 Marangoni convection.....	2
Chapter 2 LITERATURE REVIEW AND GOALS OF RESEARCH.....	6
Chapter 3 EXPERIMENT DETAILS.....	9
3.1 Experimental setup overview.....	9
3.2 Mask design.....	11
3.3 Device fabrication.....	13
3.3.1 Heater fabrication.....	13
3.3.2 Bottom chip fabrication-Hydrophilic opening.....	15
3.4 Liquid crystal calibration.....	17
3.5 Experimental procedure.....	19
Chapter 4 NUMERICAL STUDY.....	21
4.1 Introduction.....	21
4.2 Modeling.....	21
4.3 Governing equations.....	24
4.4 Multiphysics coupling.....	24
4.4.1 Heat transfer in fluids.....	24
4.4.2 Fluid flow interface.....	25
4.4.3 Marangoni effect.....	25

4.5 Initial conditions.....	25
4.6 Boundary conditions.....	25
4.7 Meshing.....	26
4.8 Solution.....	28
4.9 Result plotting.....	28
4.10 Road map.....	28
Chapter 5 RESULTS AND ANALYSIS.....	30
Chapter 6 CONCLUSIONS AND FUTURE SCOPE OF THE STUDY.....	34
REFERENCES.....	35
BIOGRAPHICAL INFORMATION.....	38

## List of Illustrations

Figure 1-1 Internal motion inside the droplet.....	1
Figure 1-2 Hotspot cooling curve.....	2
Figure 1-3 Marangoni convection.....	3
Figure 1-4 Tears of Wine.....	4
Figure 3-1 Cross sectional view of sandwiched drop between top and bottom chip.....	9
Figure 3-2 Testing station for study of Marangoni convection.....	10
Figure 3-3 Magnified view of top and bottom chip with sandwiched drop.....	11
Figure 3-4 (a) Mask showing design of ITO heater.....	12
Figure 3-4 (b) Mask showing design of Hydrophilic opening.....	12
Figure 3-5 Magnified view of heater design.....	12
Figure 3-6 Steps showing ITO heater fabrication.....	14
Figure 3-7 Steps showing hydrophilic opening fabrication.....	16
Figure 3-8 Flow chart of working of INSTEC HCS621V precision heating/cooling vacuum stage.....	17
Figure 3-9 Sandwiched IL drop with nylon seeding particles.....	20
Figure 4-1 3D CAD model used for simulations.....	22
Figure 4-2 Top view of the sandwiched drop.....	23
Figure 4-3 Side view of sandwiched drop.....	23
Figure 4-4 Figure showing fluid flow boundary conditions.....	25
Figure 4-5 Figure showing heat transfer boundary conditions.....	26
Figure 4-6 CAD model after meshing.....	27
Figure 4-7 Finer mesh on the drop.....	28

Figure 4-8 Steps involved in numerical study.....	29
Figure 5-1 Thermo-capillary convection.....	30
Figure 5-2 Flow patterns inside the drop for different heat fluxes.....	30
Figure 5-3 Flow patterns with Liquid crystal thermography.....	31
Figure 5-4 Experimental and numerical comparison of surface temperature below the bottom chip in degree Celsius for $q'' = 87.72 \text{ W/cm}^2$ .....	32
Figure 5-5 Experimental and numerical comparison of velocity along XY plane in mm/s for $q'' = 87.72 \text{ W/cm}^2$ .....	32



## List of Tables

Table 3-1 Summary of Liquid crystal calibration.....	18
Table 3-2 Currents with corresponding heat fluxes used for the experiments.....	20
Table 4-1 Dimensions for the CAD model.....	22

CHAPTER 1  
INTRODUCTION

*1.1 Motivation*

Previous experimental study [1] carried out in the area of hotspot cooling using Electrowetting on dielectric (EWOD) platform witnessed cooling due to the phase change heat transfer. It was observed when a droplet moved over the hotspot by EWOD motion there existed an internal fluid motion. Alumina particles were added to the droplet to observe the flow. Upon investigation a flow pattern was observed inside the droplet.

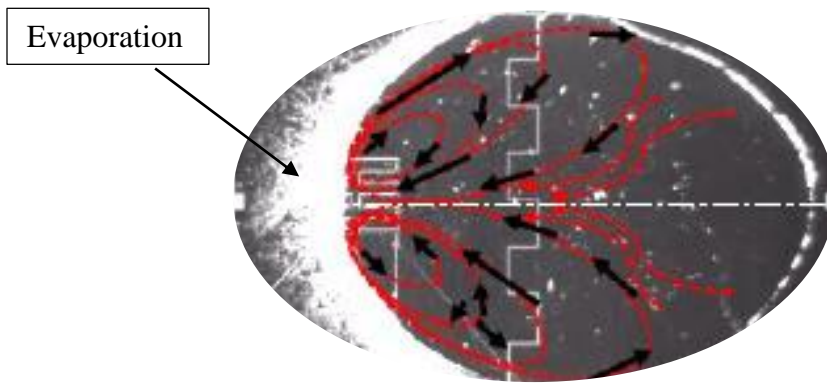


Figure 1-1 internal motion inside the droplet [1]

Since evaporation occurred along the meniscus of the drop and the mass loss by evaporation was taken account for the cause of internal flow pattern observed. In addition to evaporation, in microscale, surface tension forces are dominant, hence there could be internal flow motion caused by surface tension. Also when cooling curve (Figure 1-2) was plotted, it was observed that the more temperature drop in experimental study than in the numerical study which modeled conduction and convection only, contrary to that we observed conduction, convection, evaporation and suspected surface tension driven flow in the experimental study [1].

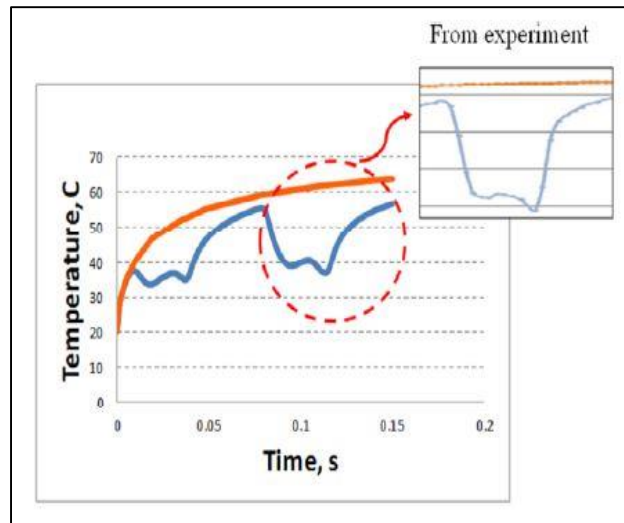


Figure 1-2 Hot spot cooling curve [2]

(Brown line represents no droplet over the hotspot, blue line represents droplet over the hotspot)

### 1.2 Marangoni convection

The surface tension at the interface between two immiscible fluids (liquid-gas or liquid-liquid) can be influenced by enforced temperature, electric fields, or existence of foreign particles. Surface tension stresses are generated under the influence of gradients in temperature, electric field, or concentration which results into interfacial flows.[3] Marangoni convection (also called Gibbs–Marangoni effect) is the mass transfer along an interface between two fluids due to surface tension gradient. If surface tension gradient is caused due temperature dependence, it is often called thermocapillary convection [4].

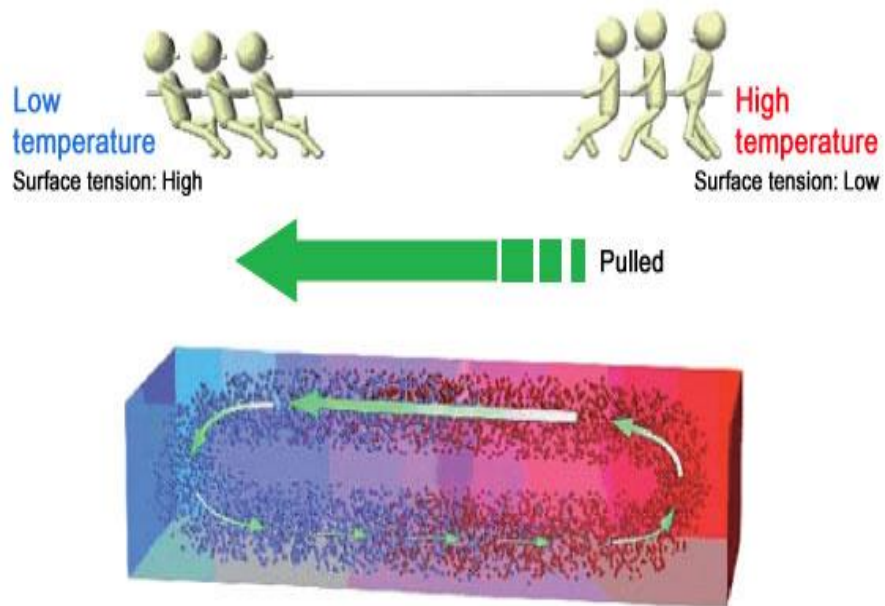


Figure 1-3 Marangoni convection [5]

Figure 1-3 is a pictorial representation of Marangoni convection which is temperature dependent in this case. The left part of the figure has low temperature hence high surface tension, while the right part has high temperature hence low surface tension, Because of surface tension gradient there exists a flow. Marangoni convection was first identified as “tears of wine” by Thompson in 1855. [6]

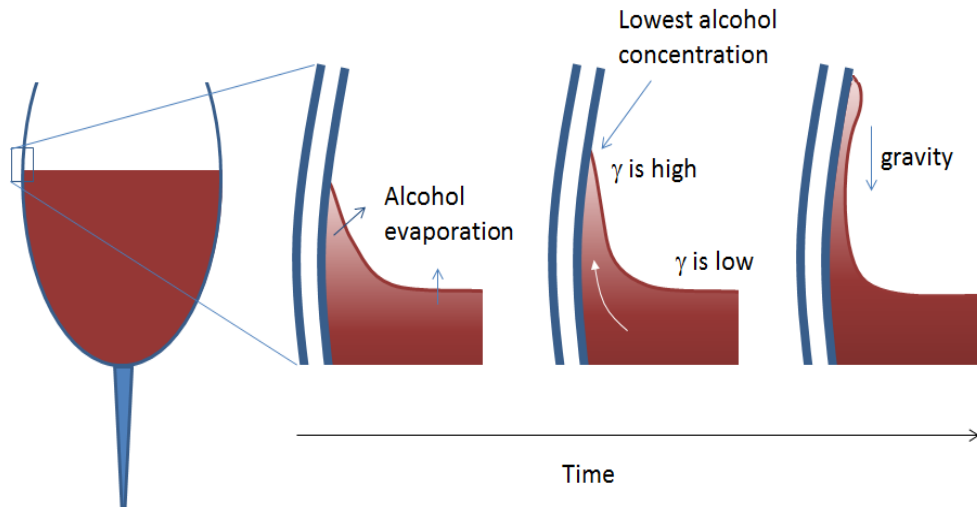


Figure 1-4 Tears of wine [7]

This phenomenon arises when wine is poured in glass and stirred lightly. We know that, wine is a mixture of water and alcohol. Also, surface tension of alcohol is lower than that of water. When we stir the glass lightly, wine adheres to the rim of the glass as shown in the Figure 1-4. As we may know that vapor pressure of alcohol is higher than that of water hence it evaporates faster than water. At the solid-liquid interface due to lower conductive resistance we observe more evaporation. Due to evaporation, the wine near the rim has less concentration of alcohol compared to wine in the bulk. Hence at the rim, surface tension is higher, which pulls the drop of wine upwards against the gravity. This continues to happen until the drop size increases to an extent where gravitational force dominates the surface tension force and the drop moves downwards.

Based on Thompson's results, Marangoni concluded that the convection could be because of surface tension gradients due to concentration or temperature gradient [8]. Hershey suggested that the higher evaporation or condensation along the border of a liquid leads to local temperature difference which causes surface tension variations and produce

liquid motion [9]. Benard performed an experiment wherein a horizontal layer of liquid is heated from below. He observed a cellular flow coupled with interface deformation [10]. This directed Rayleigh and Block to suggest different mechanisms for the convection. Rayleigh attributed the effect to buoyancy-driven convection while Block to surface tension-driven convection [11] [12]. Contrary to the natural convection, thermocapillary convection takes place in micro gravity condition i.e. the effect of body forces is negligible. This type of convection is surface tension driven convection. Microgravity condition can be achieved either by carrying out experiment in space or by reducing the length scale so that the Bond number (Bo) is less than one [13].

$$Bo = \frac{gL^2(\rho_L - \rho_g)}{\sigma}$$

Where  $g$  is acceleration due to gravity ( $m^2/s$ ),  $L$  is appropriate linear dimension (m),  $\rho_g$  is density of gas ( $kg/m^3$ ),  $\rho_L$  is the liquid density ( $kg/m^3$ ) and  $\sigma$  is interfacial surface tension (N/m). Bond number is a ratio of gravitational force to surface tension force. When bond number is less than one we can say that surface tension forces are dominant over gravitational forces. Thermocapillary effect is characterized by Marangoni number (Ma) which is given by a ratio of surface tension forces to the viscous forces [14].

$$Ma = -\frac{d\sigma}{dT} \frac{L\Delta T}{\eta\alpha}$$

Where,  $\sigma$  is surface tension (N/m),  $L$  is the characteristic length in m,  $\alpha$  is thermal diffusivity ( $m^2/s$ ) and  $\eta$  is dynamic viscosity ( $kg/(s.m)$ ) and  $\Delta T$  is temperature difference (K). Chapter 2, Literature review, talks about the research advancements in the marangoni convection.

## CHAPTER 2

### LITERATURE REVIEW & GOALS OF RESEARCH

Marangoni effect was first observed in 19<sup>th</sup> century. Since then the research has been carried out for understanding its physics and exploring its applications. As this phenomenon is observed under microgravity condition, the experiments are performed either in space or in small systems like microchannel, thin films and liquid droplet, where gravity effect is negligible. Most of the previous work done in this field has been based on non-uniform heating in numerous systems like layer of fluid, climbing film and liquid bridge [15-17]. Qualitative study of thermocapillary convection was performed using tracing particle technique and laser doppler velocimetry [18, 19]. Wozniak et al. were the first group to use particle image velocimetry (PIV) and laser-speckle velocimetry techniques to quantify the entire flow field generated by thermocapillary convection and buoyancy effect over a bubble. They observed that, with an increase in scale, buoyancy effects become dominant over surface tension effects [20, 21]. Kamatoni et al. were the first to study flow visualization using particle-tracking velocimetry in flat and curved free liquid surface. They inferred that it was more difficult for the surface flow to penetrate corner regions in curved surface compared to the flat surface case, because of the narrow passage in the pointed region. Moreover, they observed a small recirculation cell but they were not able to resolve details in this region [22]. Ruiz and Black performed a numerical analysis of the evaporation process of small droplets of diameter less than 1 mm, placed on a heated surface. They were the first to model the internal fluid motion due to thermocapillary convection in a droplet. They reported that the motion of the fluid significantly affects the thermal field in the droplet and concluded that a model without fluid motion underpredicts the evaporation rate [23]. Studies have been carried out considering combined influence of surface tension and buoyancy effects which are called as buoyant thermocapillary flow. Kirdyashkin and

group studied buoyant thermocapillary driven flow in a 2D slot and provided analytical solution for temperature and velocity profile. They also validated their results with experiments [24]. Villers and Platten observed a single steady convection cell changed to a multi-cellular pattern with an increase in marangoni number [25]. It is being reported that boiling heat transfer is strongly affected by thermocapillary convection. P.H Lin et al. used a binary mixture (alcohol and water) as a working fluid in a microchannel to study thermocapillary convection effect on boiling heat transfer. They observed that thermocapillary force supplies liquid towards the contact line which directly delays the dry-out of the liquid film resulting in enhancement of the critical heat flux (CHF) thereby enhancing boiling heat transfer [26]. Savino and Fico studied behavior of bubbles on a horizontal heated surface experimentally as well as numerically. They concluded that the heat transfer from the wall increased by a factor of 4.5-5 because of cold return flow caused by thermocapillary convection. It was seen that under low marangoni number velocity and temperature fields were found to be steady, while at very high marangoni number, oscillations were observed [27]. H. K. Dhavaleswarapu et al. investigated steady buoyant thermocapillary convection produced by differential evaporation near a meniscus in horizontal placed in microchannels of varying internal diameters. They concluded that for an evaporating meniscus in capillary tubes and for a given set of experimental conditions, a critical diameter exists such that for small diameter, the flow is driven primarily by thermocapillarity, whereas buoyancy effect sets in beyond a critical diameter leading to 3 dimensionalities in the flow [3]. Numerous thermocapillarity based devices have been proposed and developed for applications such as mixing, pumping, actuation, and sensing. As we may know that for thermocapillary convection to take place, temperature gradient is required. Most of the studies in this area use evaporation for creating temperature gradient.



Until now thermocapillary convection was studied for thin film, microchannel or sessile droplet. The aim of this research is to study pure thermocapillary convection i.e. without evaporation in a sandwiched droplet. In this study, Ionic liquid (IL) is used as a working fluid. Ionic liquid is a molten salt with very low vapor pressure hence, evaporation effect is completely eliminated [28]. The purpose of eliminating evaporation is that many studies done previously have proven the existence of Marangoni convection in an evaporating water droplet but there is no research which studies pure marangoni convection without evaporation taking place. Moreover, the contribution of Marangoni convection in hotspot cooling using an electrowetting on dielectric microfluidics needs to be evaluated. For creating temperature gradient along the drop meniscus an indium tin oxide (ITO) heater is used. This research focuses on studying marangoni convection, thermocapillary convection in this case, experimentally and validating the results obtained numerically. In this study, flow visualization with temperature field is observed experimentally for the first time. Liquid crystal thermography is used for observing temperature field. For flow visualization, contrary to the conventional method of fluorescence microscopy, polarized light microscopy is used. This method is cost effective considering the seeding particles used for flow tracking. Moreover, unlike fluorescence microscopy, this method does not need superimposing of multiple images for better contrast even in low concentration particle sample. Polarized light microscopy is a method of enhancing contrast which improves the quality of the image obtained with birefringent materials when compared to other techniques such as dark field and bright field illumination, fluorescence, differential interference contrast, phase contrast etc. [29]. Chapter 3 talks in detail about the experimental set up.

## CHAPTER 3

### EXPERIMENT DETAILS

#### 3.1 Experimental Setup Overview

In order to investigate marangoni convection, an experimental set up was designed and fabricated. In this experiment, indium tin oxide (ITO) was used as heater material. Since marangoni convection is a temperature dependent phenomenon, liquid crystal (LC) paint was used to observe the temperature profile [30]. As ionic liquid (IL) is a molten salt and does not evaporate, it is used as working fluid. An IL droplet is sandwiched between top and bottom chips, which were fabricated using standard microfabrication methods.

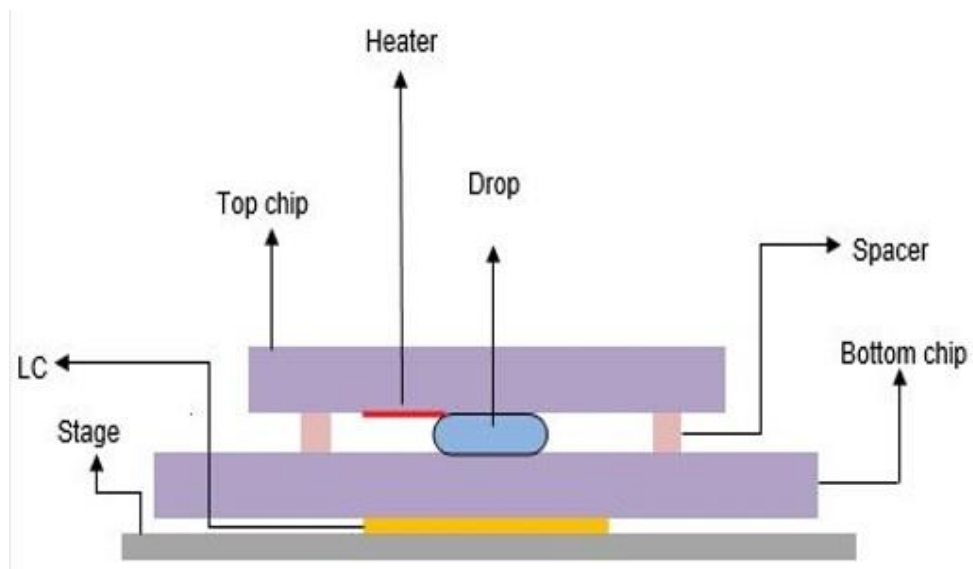


Figure 3-1 Cross-sectional view of the sandwiched drop between top and bottom chip.

In Figure 3-1, a drop is sandwiched between top and bottom chips, a heater is patterned in the top chip which provides constant heat flux. The bottom chip has a hydrophilic opening so that drop does not move from its position after keeping top chip over it. The top and bottom chip are both 0.7 mm in width. A spacer of thickness 0.180 mm is

placed between the top and the bottom chips. Liquid crystal layer is placed beneath the bottom chip to observe temperature gradient across the drop. The flow visualization in the drop and the temperature profile on the LC is observed and captured with the help of a Nikon LV 150 microscope with a camera integrated in it.

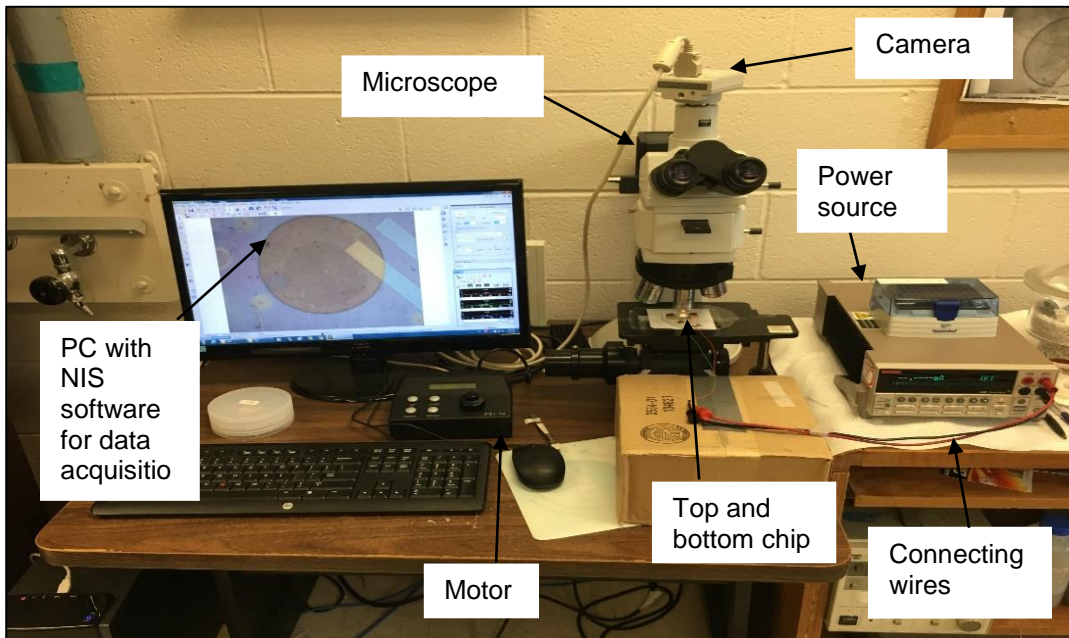


Figure 3-2 Testing station for study of marangoni convection

The experimental setup is as shown in the Figure 3-2. Indium tin oxide thin film heater is connected to the Keithly power source with the help of 30 gauge wire. These wires cannot be soldered on ITO contact pads directly. Hence silver epoxy is pasted on contact pads over which copper strips are attached. The top chip is then kept inside an oven at 70 °C for 6 hours. This makes the silver epoxy hard so that it can adhere well with the copper strip. At this stage, wires are soldered over the copper strips. Kapton tape is used as spacer and its thickness is measured using a profilometer. Phosphonium based IL (triethyl (tetradecyl) phosphonium bis (trifluoromethanesulfonyl) imideis) is used as a

working fluid. For flow visualization, particles are seeded in the ionic liquid. An exhaustive research on seeding particle is done considering the size, density and camera compatibility for tracing the particles. Nylon seeding particles (TSI inc., 4.0  $\mu\text{m}$  mean diameter, 1.0 g/cc density) are chosen as the best fit for this experiment. Keithly power source is used to supply current in mA. A motor is used to move the stage in Z direction on which the device rests. Approximate temperature profile along the bottom chip is observed with the help of LC. The flow visualization and temperature profile data are recorded with the help of NIS software.

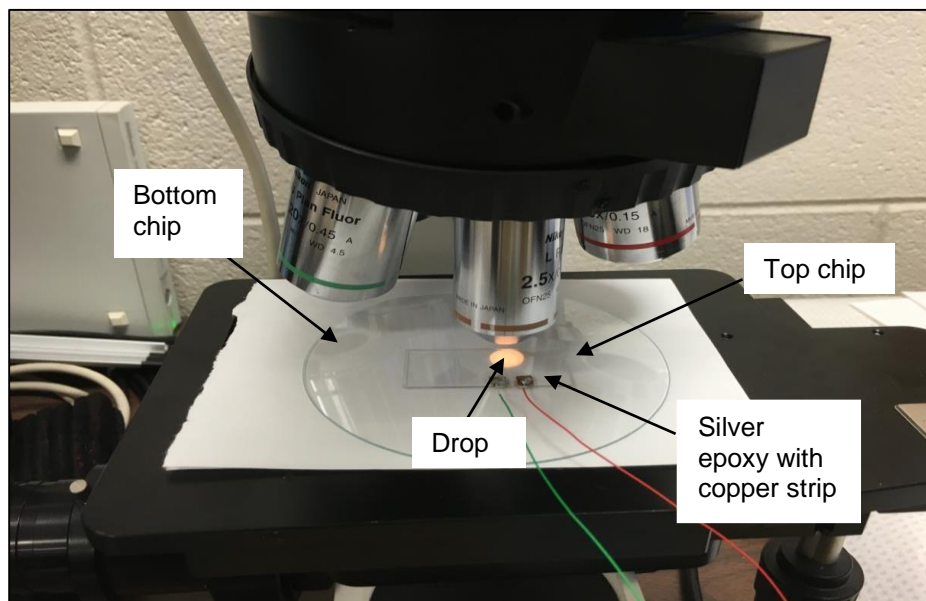


Figure 3-3 Magnified view of top and bottom chip with sandwiched drop

### 3.2 Mask Design

As mentioned in the beginning of this chapter top chip and bottom chips were fabricated using standard microfabrication methods with facilities UTA NanoFab. Figure 3-4 (a) shows the mask used for ITO heater fabrication and Figure 3-4 (b) shows the

mask used for fabricating the hydrophilic opening. These masks were used for top chip and bottom chip, respectively.

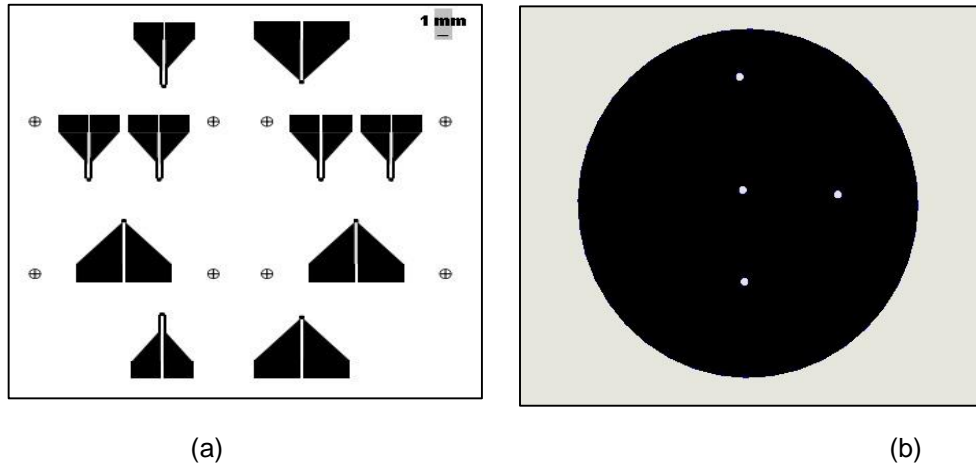


Figure 3-4 (a) Mask showing design of ITO heater and (b) mask showing hydrophilic opening, used in photolithography for device fabrication



Figure 3-5 Magnified view of heater design

The mask for heater was designed using L-Edit software by Tanner EDA. The final circuit design was exported to GDS (Graphic Data System) file type and was then converted to PostScript (PS) format using LinkCAD software. The PS format helps us to view the final design which was similar to PDF format. The PS file was sent to a mask printing company, CAD/Art Services Inc., Oregon. For ease of design, the bottom chip mask was designed

using SolidWorks software. This mask was printed on transparency sheets using Brother HL – 2170W series printer. Five transparency sheets were printed and were stacked together. These masks were used in the photolithography process. Photolithography is a microfabrication process which is explained in detail in next section.

### *3.3 Device Fabrication*

The fabrication steps include cleanroom MEMS fabrication process; spin-coating, photolithography, developing, wet etching, reactive ion etching (RIE), photoresist (PR) stripping and baking. A four-inch ITO wafer was used for the top chip fabrication while a four-inch glass wafer was used for fabrication of the bottom chip. Prior to any fabrication process, a thorough cleaning of wafer was done. Acetone, isopropyl alcohol and methanol were used as cleaning agents. Furthermore, deionized (DI) water was used for rinsing the wafer. After rinsing, the wafer was blow dried with nitrogen gas and dehydrated on a hot plate (Isotemp, Fisher Scientific) at 150 °C.

#### *3.3.1 Heater Fabrication*

Spin coating is a process of deposition of thin films of uniform thickness on a substrate by spinning it. Prior to spin coating of PR over the wafer, Hexamethyldisilazane (HMDS) was spin coated. HMDS is a colorless solution which offers better adhesion of PR to an ITO wafer. As per the mask design, a positive PR was used. S1813 was used as a PR in this fabrication. HMDS was carefully poured on a wafer and spun using a customized recipe. This recipe involved spinning the wafer to 500 rpm for the first 5 seconds and then ramping it up to 4000 rpm at a rate for 900 rpm/s. The wafer was spun for the next 30 seconds at constant speed. After spin coating of HMDS the wafer was soft baked at 110 °C for 1.5 min.

The same recipe is used for spin coating PR followed by a soft bake at 115 °C for a min. After spin coating process, UV exposure was done. The fabrication process flow is shown in figure 3-6

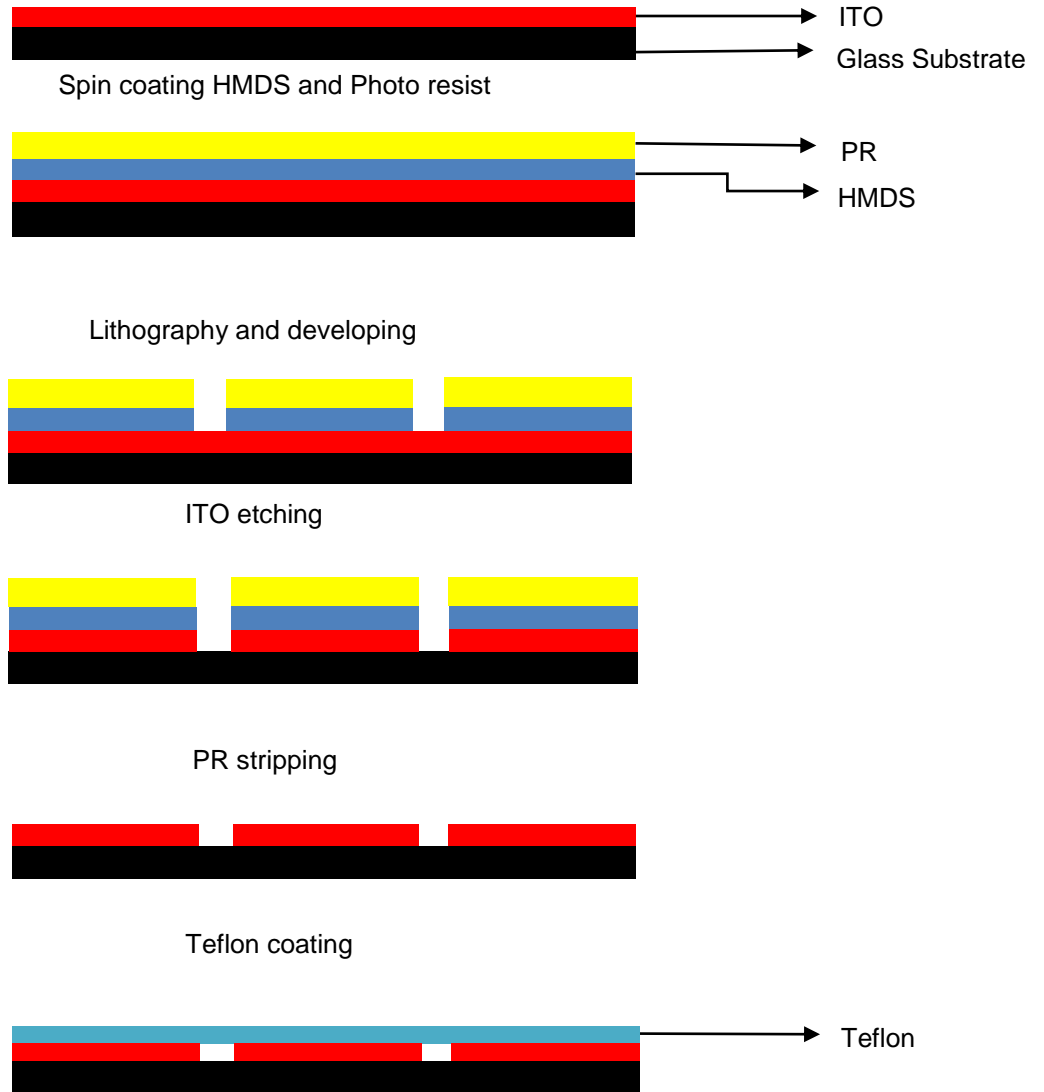


Figure 3-6 Steps showing ITO heater fabrication process

Photolithography is used to remove selective parts of PR. A lithography mask (Figure 3-4) is used in this process. An ITO wafer spin-coated by HMDS and PR is subjected to high energy UV exposure for 7 seconds.. UV light passes through the blank area on the mask

and does not pass through the printed black portion. This changes the chemical properties of PR (sensitive to light) which affects only the blank area through which it passes. A post exposure bake was done at 115 °C for one minute to harden the PR which is left on the wafer. After this stage, developer solution (MF-319) was used to dissolve and remove part of the PR which was exposed to UV rays, this left behind the unexposed PR which formed the pattern. A post developing bake was carried out before etching, so that, etching does not affect the PR layer. An etchant solution comprised of HNO<sub>3</sub>, HCl and DI water in proportion, 1:8:15 was used. To catalyze the process, etchant was heated up to 55 °C. This process was carried out for 5 mins. Lastly, a PR stripper solution was used to remove the baked PR to expose the chip with ITO patterned heater. This heater was spin-coated with Teflon using a custom recipe, which involved spinning the wafer to 600 rpm for the first 5 seconds and then ramping it up to 2000 rpm at a rate for 500 rpm/s. The wafer was spun for the next 30 seconds at constant speed. After spin-coating, the wafer was baked at 50 °C for 5 min, 150 °C for 10 min and 180 °C for 5 min.. This step helped to remove the Teflon solvent and anneal it.

### *3.3.2 Bottom chip fabrication: Hydrophilic opening*

Since the drop moves from its position on the bottom chip when it is being sandwiched, a hydrophilic opening is fabricated to cease its movement. Similar to the heater fabrication a thorough cleaning of a glass wafer was carried out. The wafer was dehydrated at 150 °C for 5 min. The fabrication process is shown in Figure 3-7.



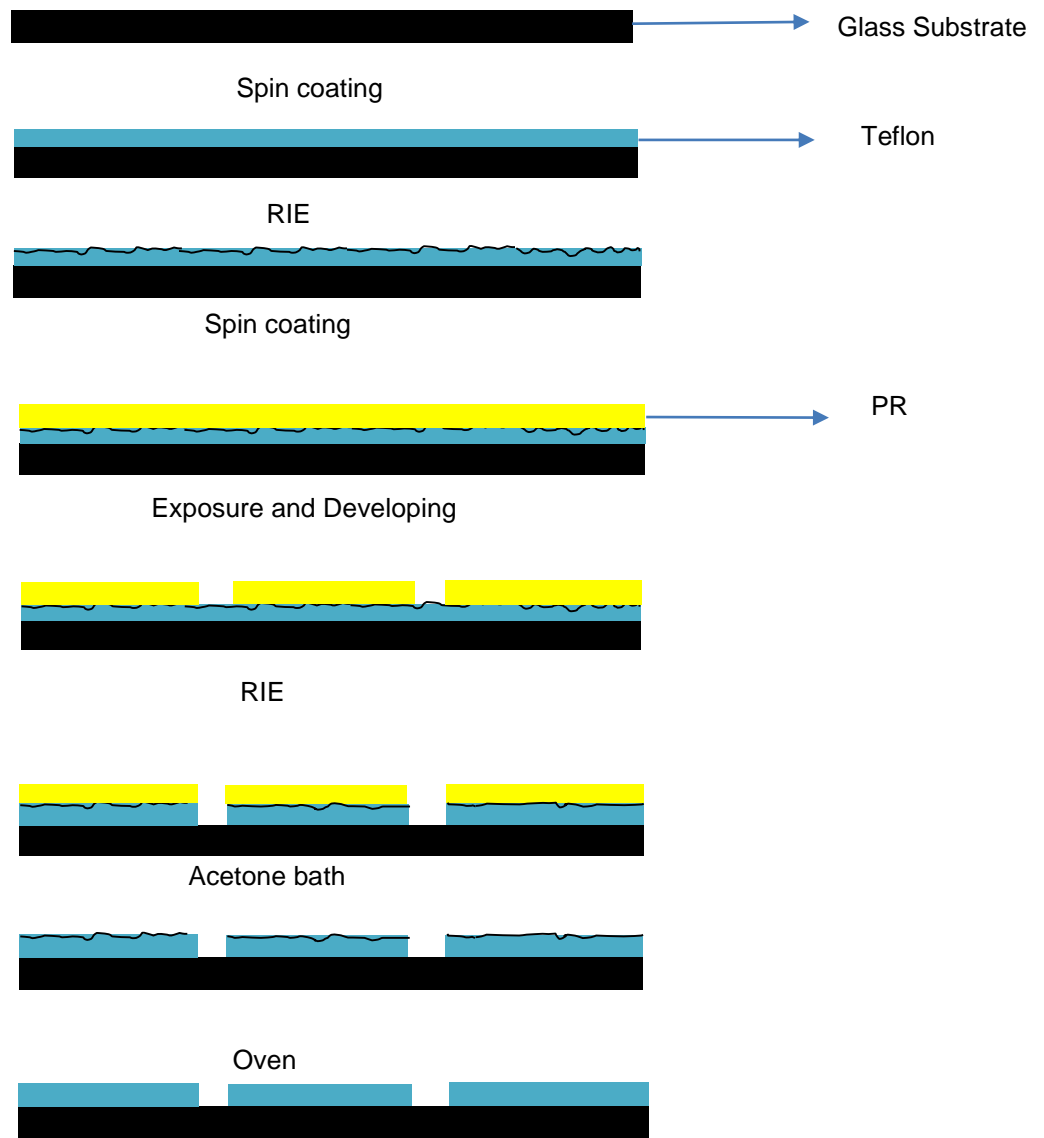


Figure 3-7 Steps showing hydrophilic opening fabrication

After dehydration, Teflon was spin-coated on the glass wafer using same custom recipe used in heater fabrication followed by baking. After this step reactive ion etching (RIE) was carried out for 8 seconds with an intensity of 160 W, 30 sccm Argon gas to make the Teflon surface rough. This was done to improve the adhesion of PR over the Teflon. PR (S1813) was spin-coated over this wafer (custom recipe, same as described in heater fabrication).

A soft bake at 115 °C for 1 min was done. Photolithography as discussed in the heater fabrication section was carried out. A post exposure bake was carried out at 110 °C for 1 min. After this step, a developer solution, MF 319 was used to dissolve and remove the parts of PR exposed to UV rays. RIE was performed to remove Teflon from the opening (blank region in Figure 3-4b). Time duration for RIE was 1 hour 30 min at 200 W and 20 sccm Argon gas. After RIE, Teflon is removed from the openings which were exposed to UV rays, although a layer of PR does remain over the other region. This wafer is immersed in an acetone bath for 15 – 20 min to remove the PR. Finally we got a device which had hydrophilic openings and the rest of the region is covered by Teflon. This device was kept in an oven at 200 °C for an hour to make the Teflon surface smooth.

### 3.4 Liquid crystal calibration:

To get temperature profile across the bottom chip beneath the drop, it is not useful to use resistance temperature detector (RTD), which would give temperature at specific points. Here, we are interested to obtain a thermal map of the bottom chip. This would represent the temperature gradient along the liquid drop placed just above the bottom chip. Hence, we use LC to obtain the temperature distribution on the bottom chip surface. Liquid crystal was calibrated using INSTEC HCS621V precision heating vacuum stage.

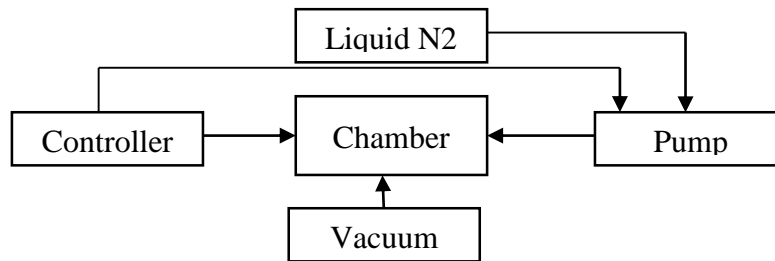


Figure 3-8 Flow chart of working of INSTEC HCS621V precision heating/cooling vacuum stage.

Liquid crystal layer is placed in the chamber and the chamber is closed so that there is no heat transfer between the system and environment. Vacuum is used to isolate the system. The stage on which the LC rests, works on joule heating principle. The chamber has a glass pane to observe the sample resting on the stage. A PID controller is used to control the heating/cooling of the stage. Liquid nitrogen can be used to quickly cool the stage. The film of LC is initially black in color and changes its color for a specific temperature range. Initial temperature of the stage was 25°C. The temperature of stage is increased to 35°C and the color in the LC film was observed. Until 40 °, there was no color change in LC. At 40.5 °C, change in color was observed. This experiment was carried out till the LC showed black color i.e. beyond the operating temperature of the liquid crystal thermography. The table below gives detailed calibration results.

Table 3-1 Summary of Liquid Crystal calibration

Temperature (°C)	Color
30-40	Black
40-40.5	Red
40.5-41.5	Orange
41.5-42	Yellow
42.0-45	Green
45.5-49.5	Blue
50-54	Violet
54.5 and above	Black

### *3.5 Experiment Procedure*

The set up for marangoni convection experiments consisted of a Nikon microscope integrated with a camera for flow visualization, a computer which had NIS software for capturing and recording the data, a Keithly power source to supply current, top chip with an ITO heater, bottom chip with hydrophilic opening, kapton tape for spacer gap, alligator clip and 30 gauge wires for electrical connections, liquid crystal for temperature measurement, ionic liquid as working fluid and nylon seeding particles.

The computer which had the camera/microscope software along with the microscope was powered on. Nylon seeding particles were added to ionic liquid solution and properly mixed using a vortex genie mixer. This solution was kept in a desiccator so that ionic liquid does not absorb water and change its properties. A Keithly power source was used to supply current to the ITO heater. A bottom chip with hydrophilic opening was placed on the microscope stage. LC is placed beneath the bottom chip to observe temperature profile. Four pieces of kapton tapes are attached to the bottom chip to create spacer gap between top and bottom chip. A drop of IL, mixed with nylon seeding particles is dispensed on the hydrophilic opening with the help of Eppendorf dispenser. Top chip was placed over the bottom chip to sandwich the drop. ITO heater on the top chip is connected with a 30 gauge wire which is connected to the alligator clips and these clips were connected to the power source.

After sandwiching the drop between two plates, the top chip is adjusted such that the heater is placed over some part of the meniscus as shown in the Figure 3-9. This is the most of the difficult part, since the drop moves from its position under the heater. Hence, hydrophilic opening is created to fix the position of the drop. A desired current and voltage on the power source was set and the current was passed through the circuit

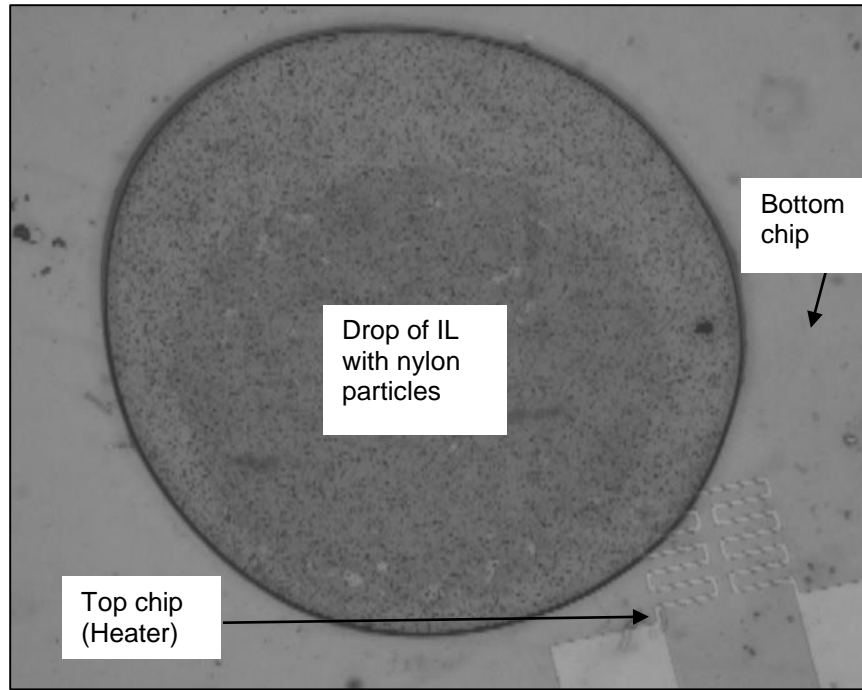


Figure 3-9 Sandwiched IL drop with nylon seeding particles

As soon as the current was passed there was temperature gradient along the meniscus which led to surface tension gradient which resulted in marangoni convection. The flow and temperature data was being recorded with the help of NIS recorder. The experiment was conducted for three heat fluxes.

Table 3-2 Currents with corresponding heat fluxes used for the experiments

Electric current (mA)	Resistance ( $\Omega$ )	Area ( $\text{cm}^2$ )	Heat flux( $\text{W}/\text{cm}^2$ )
8	1523	$2.5 \times 10^{-3}$	38.98
10	1523	$2.5 \times 10^{-3}$	60.92
12	1523	$2.5 \times 10^{-3}$	87.72

## CHAPTER 4

### NUMERICAL STUDY

#### *4.1 Introduction*

In order to validate the experimental results, numerical simulations were done. COMSOL Multiphysics, a finite element analysis (FEA) solver and simulation commercial software was used for this study. Finite element analysis, also known as finite element method (FEM) is a numerical approach for calculating approximate solution of a problem by applying required loads and boundary conditions. The numerical methods help to give approximate values of the unknowns at discrete number of points in the continuum. Discretization is the process of modeling a body by dividing it into an equivalent system of smaller bodies (also known as finite elements) which are interconnected at points common to two or more elements (nodes) and/or boundary lines and/or surfaces. In the finite element method, rather than solving the problem for the entire body in one operation, we develop the equations for each finite element and combine them to get the solution of the entire system [31].

#### *4.2 Modeling*

A 3-D, single-phase model was built using COMSOL Multiphysics software. Microfluidics and Heat transfer modules are used in these simulations. The first step involved in this study is to choose space dimension followed by selecting physics involved in the problem. For space dimension a 3-D entity is chosen. A 3-D CAD model is built in COMSOL which emulates the experimental set up.

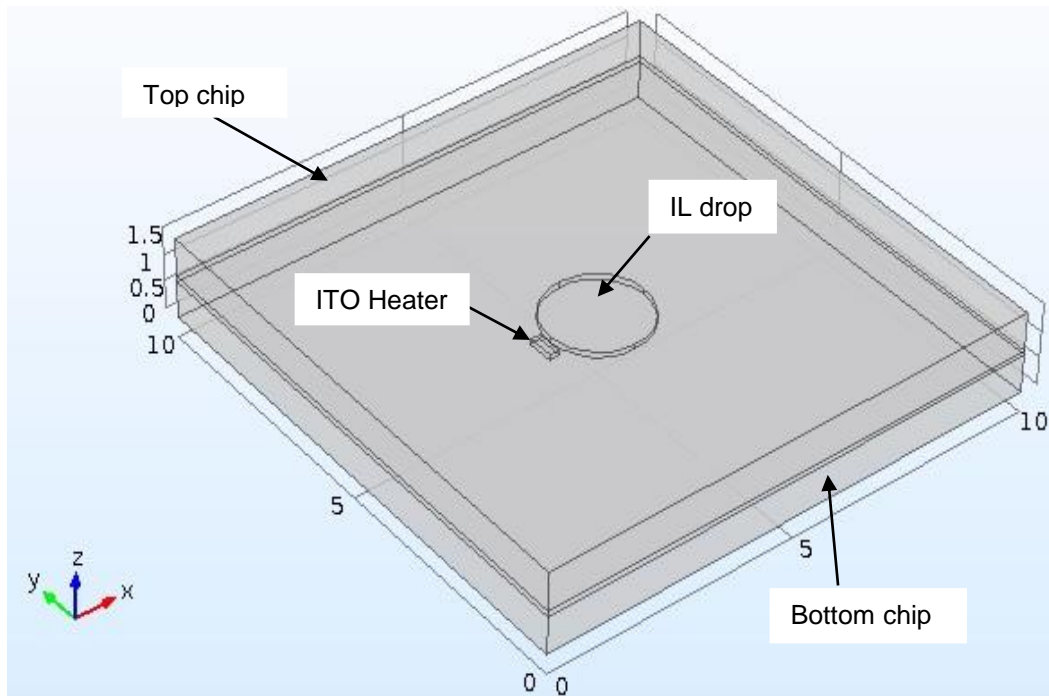


Figure 4-1 3D CAD model used for simulations

As seen in Figure 4-1, an IL drop is sandwiched between a top and bottom plate. An ITO heater is used to create temperature difference along the meniscus. The dimensions of the CAD model are given in detail in the table below.

Table 4-1 Dimensions for the CAD model

Part name	Length (mm)	Breadth (mm)	Height (mm)
Top chip	10	10	0.5
Bottom chip	10	10	0.5
Gap (Air)	10	10	0.1
Heater	0.2	0.5	0.1
Drop	Diameter (mm)		Height (mm)
	2		0.1

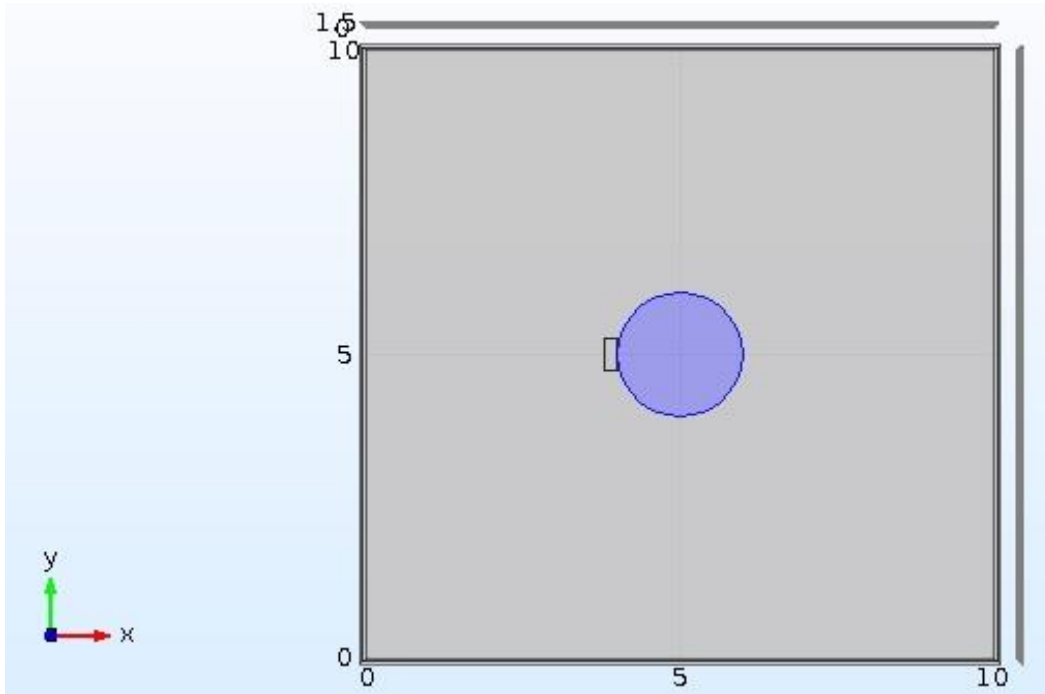


Figure 4-2 Top view of the sandwiched drop

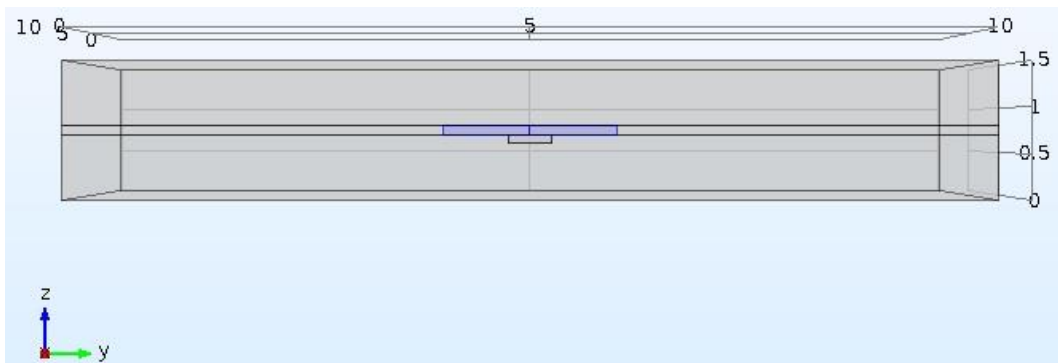


Figure 4-3 Side view of sandwiched drop

Figure 4-2 and 4-3 show top view and side view of the sandwiched drop. After the geometry is set up, material properties are assigned to the CAD model from the COMSOL library. Top and bottom chips are considered as silica glass and the gap in between these chips



is considered as air. For the drop, properties of IL are assigned. Moreover parameters like density, contact angle, temperature etc. are defined in this step

#### 4.3 Governing equations

As we know Marangoni convection is a combination of two physics viz. fluid dynamics and heat transfer, hence these two physics are chosen for the study. Furthermore, in fluid flow, single phase, laminar flow is considered, while in heat transfer, since we are interested to know the temperature field along the drop surface, heat transfer in fluids interface is chosen. In the previous step geometry is built up and material properties are assigned to it. At this step, heat transfer and fluid flow physics is being setup. Moreover boundary conditions are defined in this stage. For fluid flow, an incompressible, time dependent Navier-Stokes equation is used.

$$\rho \frac{\partial u}{\partial t} + \rho(u \cdot \nabla)u = \nabla \cdot [-pI + \mu(\nabla u)^T] + F$$

$$\rho \nabla \cdot (u) = 0$$

For Heat transfer, Energy equation is used.

$$\rho C_p \frac{\partial T}{\partial t} + \rho C_p u \cdot \nabla T + \nabla \cdot q = Q + Q_p + Q_{vd}$$

$$q = -k \nabla T$$

#### 4.4 Multiphysics coupling

##### 4.4.1 Heat transfer in fluids

For the fluid domain, i.e. for a drop, conduction and convection heat transfer is considered, while for solid domain, i.e. for air, heater, top and bottom chip, conduction is considered. As for the velocity field (u,v,w) single phase laminar flow is considered.

#### 4.4.2 Fluid flow interface

The properties viz. density and viscosity are the functions of temperature. Hence change in these properties leads to change in temperature in heat transfer in fluids.

In this way heat transfer and fluid flow are coupled.

#### 4.4.3 Marangoni effect

A default marangoni effect was provided along the drop meniscus. Due to the temperature gradient shear stress is induced. The below written equation states that shear stress is directly proportional to the temperature gradient [4].

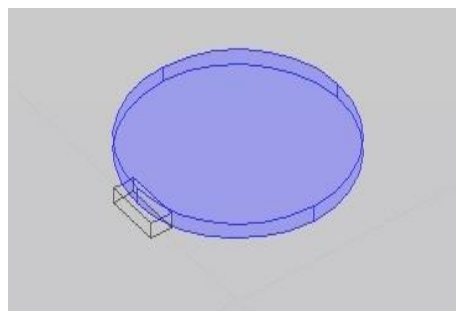
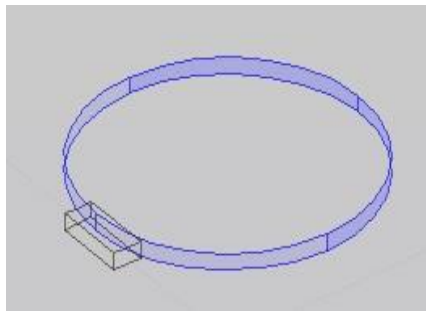
$$\eta \frac{\partial u}{\partial y} = \gamma \frac{\partial T}{\partial x}$$

#### 4.5 Initial conditions

Velocity is considered as zero, atmospheric pressure and temperature were considered.

#### 4.6 Boundary conditions

For fluid flow domain, no slip boundary condition was provided on top and bottom part of the drop, while slip boundary condition was provided along the meniscus of the drop.

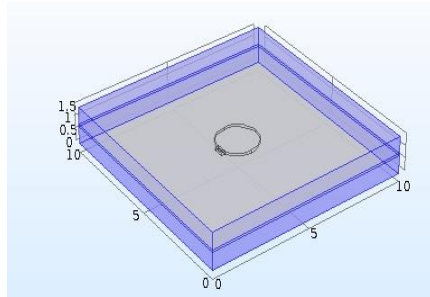


$$\mathbf{u} \cdot \mathbf{n} = 0, \text{slip}$$

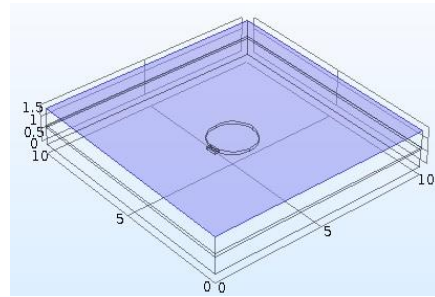
$$\mathbf{K} - (\mathbf{K} \cdot \mathbf{n})\mathbf{n} = 0, \mathbf{K} = [\mu(\nabla \mathbf{u} + (\nabla \mathbf{u})^T)]\mathbf{n}, \text{no slip}$$

Figure 4-4 Figure showing fluid flow boundary conditions

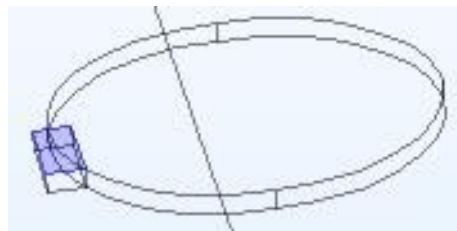
For heat transfer domain, sides of top and bottom chip were provided insulation, whereas heat flux was provided on the heater and natural convection is considered on the top chip



$$-n \cdot q = 0, \text{ Insulation}$$



$$-n \cdot q = q_0, q_0 = h(T_{ext} - T), \text{ Convection}$$



Heat flux (Constant)

Figure 4-5 Figure showing heat transfer boundary conditions

#### 4.7 Meshing

We are familiar with the process of discretization as discussed in the introduction of this chapter. Meshing is the process of discretization of the geometry. In this model we have used free mesh which is locally refined i.e. finely meshed at the area of interest. If the entire geometry is finely meshed in that case we need more computational power and time compared to locally refined mesh. Moreover some areas in the model are not of our interest, hence they can be coarsely meshed as no

important data is to be obtained from those areas. The tetrahedral mesh elements were used in this case. Figure 4-6 shows a complete meshed model while Figure 4-7 shows finer mesh on the drop. The dark area on the model represents finer mesh, while the other areas represent coarse mesh. As we are interested in observing the velocity and temperature profile in the drop, hence we use a finer mesh for it. While the top chip, bottom chip, gap and heater are coarsely meshed. In this model there are 2,52,840 domain elements.

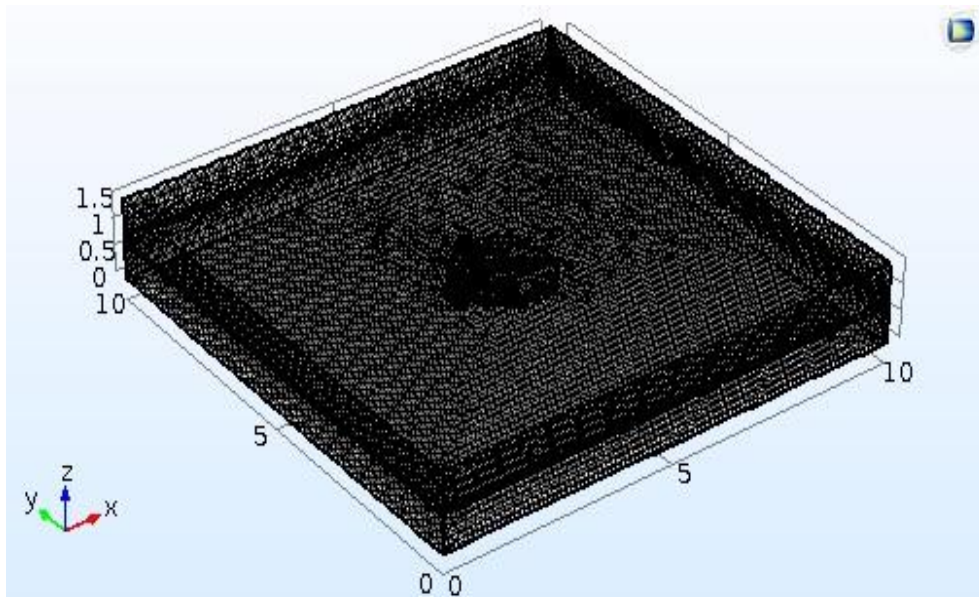


Figure 4-6 CAD model after meshing

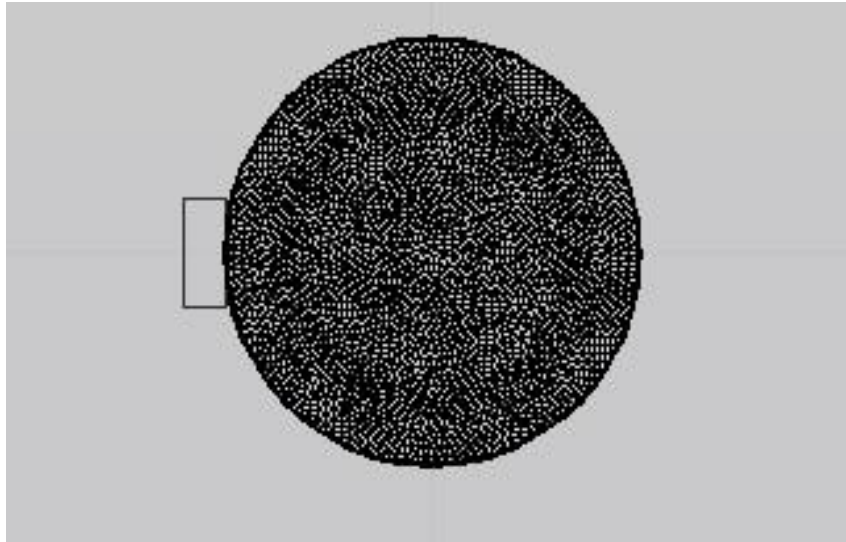


Figure 4-7 finer mesh on the drop

#### *4.8 Solution*

After meshing, with the help of an integrated COMSOL MULTIPHYSICS solver we compute the solution. Since this is time dependent study hence we have to define the time (name of solver).

#### *4.9 Results Plotting*

Once the solution is computed, we plot the results. In this study we plot the temperature and velocity profile along the drop. We also plot the streamlines.

#### *4.10 Road Map*

Figure 4-8 shows all the steps performed from start to the end to compute the numerical solution

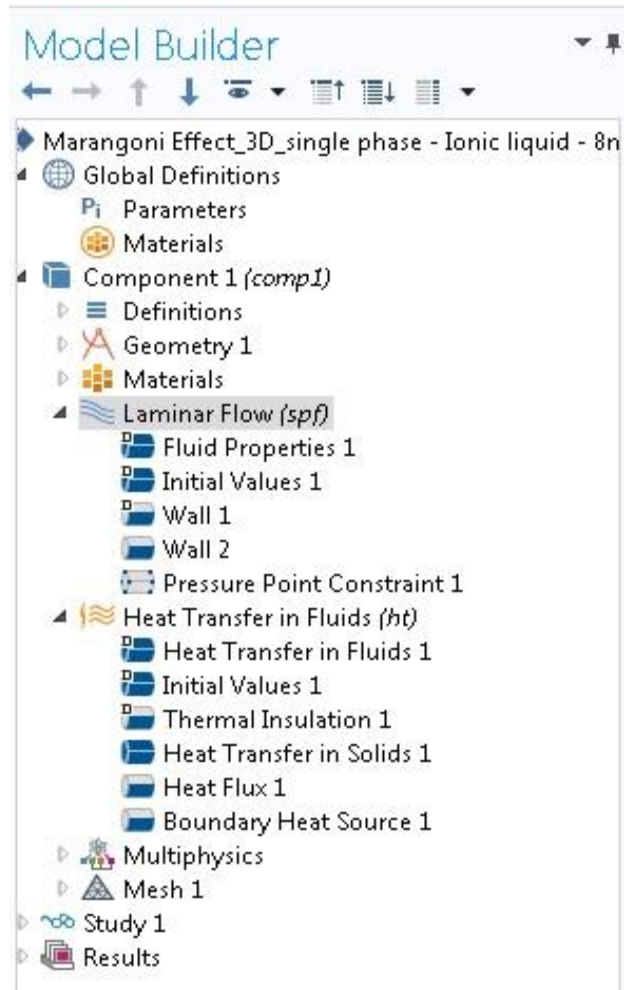


Figure 4-8 Steps involved in numerical study

Chapter 5 talks about the numerical and experimental results and analysis.

CHAPTER FIVE  
RESULTS AND ANALYSIS

Upon supply of current to the ITO heater, flow patterns were observed inside the drop.

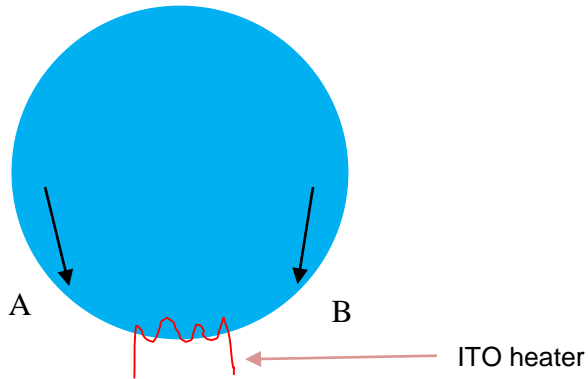
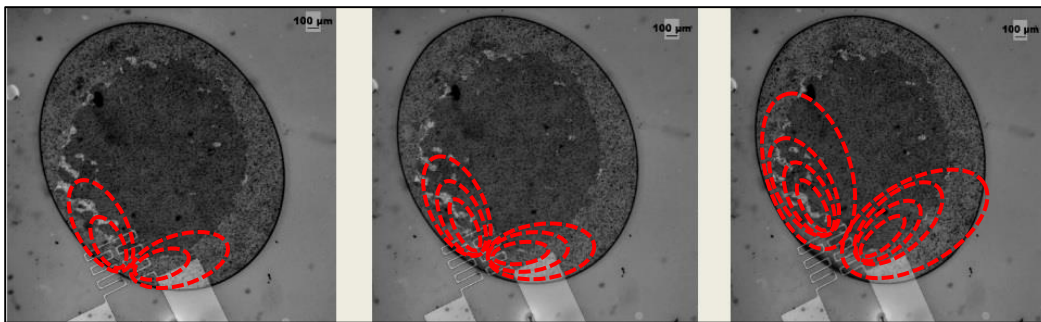


Figure 5-1 Thermocapillary convection

Temperature at the heater region is higher compared to temperature away from the heater i.e. (around point A and B). We know that surface tension is a function of temperature and it decreases with increase in temperature. Hence the surface tension at point A and B is higher compared to the surface tension around the heater region, thus causing a gradient and thereby creates a flow. Due to the mass conservation there is a recirculation of the flow.



$q'' = 38.98 \text{ W/cm}^2$

$q'' = 60.92 \text{ W/cm}^2$

$q'' = 87.72 \text{ W/cm}^2$

Figure 5-2 Flow patterns inside the drop for different heat fluxes

Flow pattern video link: <https://youtu.be/esCBCSANzZ8>

Flow visualization is done with the help of Nikon LV150 camera. The heat fluxes considered in this case were 38.98, 60.92 and 87.72 W/cm<sup>2</sup>. It was observed that with increase in the heat flux the temperature gradient along the meniscus increases which results into more vigorous flow. A similar set of experiments were performed using LC for observing the thermal map. Temperature map or thermal map was observed only for heat flux 87.72 W/cm<sup>2</sup>. As we know that the liquid crystal operates within a certain range of temperature, moreover ITO heater was kept on for 20 s in all three heat flux cases. It was observed that the temperature to instigate change in LC color was incurred by heat flux value of 87.72 W/cm<sup>2</sup>.

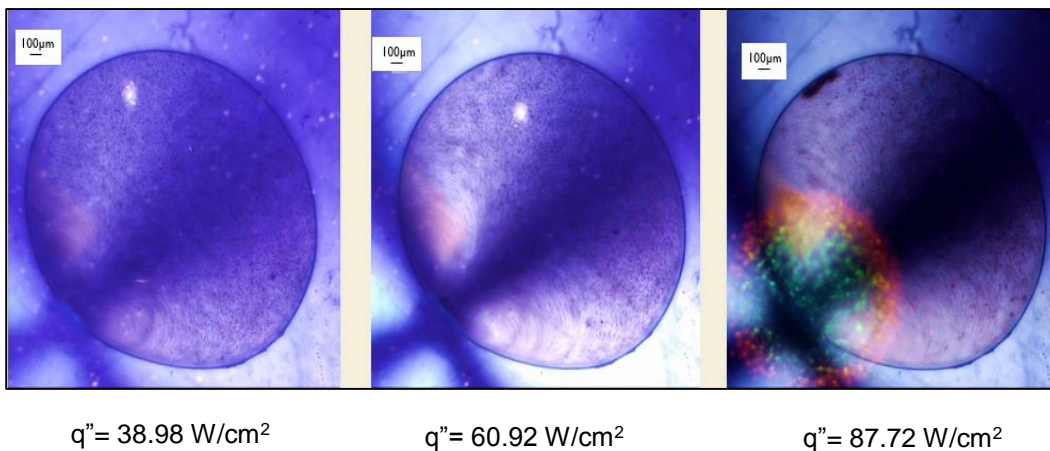


Figure 5-3 Flow pattern with Liquid crystal thermography

Flow pattern with LCT video link: <https://youtu.be/BqGj-npX1s0>

A numerical study is carried out to validate experimental results. Liquid crystal sheet is placed beneath the bottom chip, below the droplet. As mentioned earlier a thermal map is observed along the meniscus of the droplet. With the help of COMSOL MULTIPHYSICS thermal map is plotted below the bottom chip.



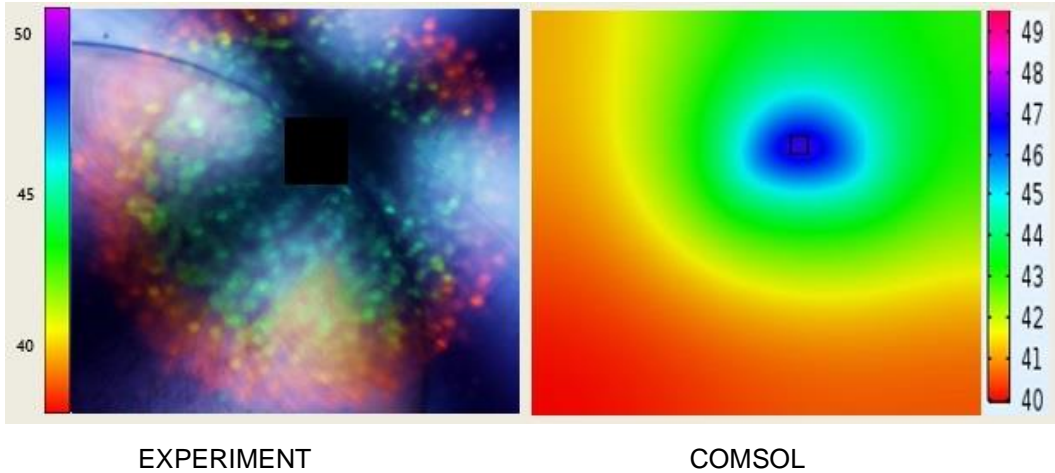


Figure 5-4 Experimental and numerical comparison of surface temperature below the bottom chip in degree Celsius for  $q'' = 87.72 \text{ W/cm}^2$

As seen in Figure 5-4 a similar temperature gradient is obtained by experiments and numerical study using COMSOL MULTIPHYSICS. Temperature found at heater by experiments is around  $49 \text{ }^\circ\text{C}$  while temperature obtained at the same region by COMSOL is  $48 \text{ }^\circ\text{C}$ . For velocity from experiments, a micro particle image velocimetry ( $\mu$ -PIV) is done using Phantom software.

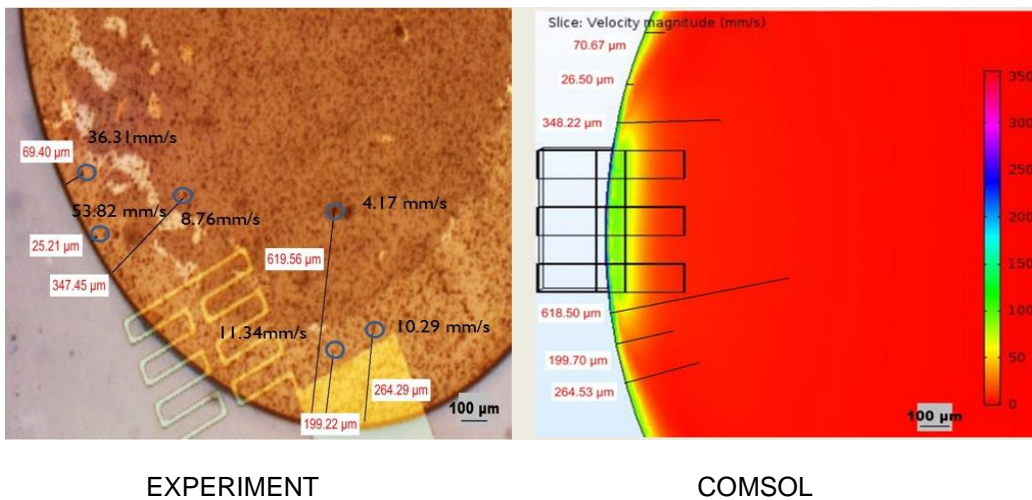


Figure 5-5 Experimental and numerical comparison of velocity along XY plane in mm/s for  $q'' = 87.72 \text{ W/cm}^2$

It was observed that the experimental and numerical velocities obtained are in good agreement with each other. It was also observed that velocity for  $q'' = 87.72 \text{ W/cm}^2$  is highest (maximum velocity is 350mm/s).

## CHAPTER SIX

### CONCLUSIONS AND FUTURE SCOPE

An experimental and numerical study of marangoni convection (thermocapillary convection) in a sandwiched droplet is carried out. The conclusions drawn from this study are as follows:

- 1) Marangoni convection also has a contribution in hotspot cooling with a droplet in Electrowetting on dielectric microfluidics.
- 2) Pure marangoni convection i.e. without any evaporation is studied experimentally using ionic liquid with micro-particles.
- 3) Experimental results are in good agreement with the numerical study carried out using COMSOL MULTIPHYSICS.
- 4) As heat flux increases, temperature gradient increases thus increasing the surface tension gradient which increases the velocity.
- 5) As we may know mixing is a problem in microscale since Reynold number is very small in this scale, marangoni convection can be used for mixing.
- 6) A numerical study including conduction, convection and marangoni convection should be carried out for hotspot cooling research, results can be compared with the hotspot cooling curve. Contribution of Marangoni convection in hotspot cooling can be determined.

## REFERENCES

- [1] G. Bindiganavale, "Study of Hotspot Cooling for Integrated Circuits Using Electrowetting on," no. May, 2015", Ph.D, The University of Texas at Arlington, 2015.
- [2] M. Nahar, S. Bindiganavale, J. Nikapitiya and H. Moon, "Numerical Modeling of 3D Electrowetting Droplet Actuation and Cooling of a Hotspot", in *COMSOL CONFERENCE*, Boston, 2015, pp. 1-7.
- [3] H. Dhavaleswarapu, P. Chamarthy, S. Garimella and J. Murthy, "Experimental investigation of steady buoyant-thermocapillary convection near an evaporating meniscus", *Physics of Fluids*, vol. 19, no. 8, p. 082103, 2007.
- [4] V. Levich, *Physicochemical hydrodynamics*. Englewood Cliffs, N.J.: Prentice-Hall, 1962.
- [5] Yasuhiro Kamotani (2013, April 13) *Marangoni:Experiment - International Space Station - JAXA* [Online]. Available:<http://iss.jaxa.jp/en/kiboexp/theme/first/marangoni/>.
- [6] J. Thompson, "On certain curious motions observable at the surfaces of wine and other alcoholic liquors", *Philosophical Magazine*, no. 10, p. 330, 1855.
- [7] B. Costa, "Tears of Wine and the Marangoni Effect", *comsol blog*, 2015.
- [8] C. Marangoni, "On the Expansion of a Drop of Liquid floating on the surface of another liquid", Pavia, 1865.
- [9] A.V.Hershey, "Ridges in a liquid surface due to the temperature dependence on surface tension,"*Physical Review*, 56, 204, 1939
- [10] H.Benard, "Les tourbillions cellularities dans une nappe liquide," Rev. Gen. Sci, Pures Appl.11, 1261, 1900
- [11] L. Rayleigh, "LIX. On convection currents in a horizontal layer of fluid, when the higher temperature is on the under side", *Philosophical Magazine Series 6*, vol. 32, no. 192, pp. 529-546, 1916.
- [12] M. Block, "Surface Tension as the Cause of Bénard Cells and Surface Deformation in a Liquid Film", *Nature*, vol. 178, no. 4534, pp. 650-651, 1956.
- [13] C. Chun and Wuest, "A micro-gravity simulation of the Marangoni convection", *Acta Astronautica*, vol. 5, no. 9, pp. 681-686, 1978.
- [14]J. Pearson, "On convection cells induced by surface tension", *J. Fluid Mech.*, vol. 4, no. 05, p. 489, 1958.

- [15] L. Scriven and C. Sterling, "On cellular convection driven by surface-tension gradients: effects of mean surface tension and surface viscosity", *J. Fluid Mech.*, vol. 19, no. 03, p. 321, 196
- [16] A. Hosoi and J. Bush, "Evaporative instabilities in climbing films", *J. Fluid Mech.*, vol. 442, 2001.
- [17] J. Xu and S. Davis, "Convective thermocapillary instabilities in liquid bridges", *Physics of Fluids*, vol. 27, no. 5, p. 1102, 1984.
- [18] G. Pétré, M. Limbourg-Fontaine and J. Legros, "Preliminary results of Texas 8 experiments on effects of surface tension minimum", *Acta Astronautica*, vol. 12, no. 3, pp. 203-206, 1985.
- [19] D. Villers and J. Platten, "Separation of Marangoni convection from gravitational convection in earth experiments", *Physicochemical hydrodynamics*, vol. 8, no. 173, 1987.
- [20] K. Wozniak, G. Wozniak and T. Roesgen, "Particle-image-velocimetry applied to thermocapillary convection", *Experiments in Fluids*, vol. 10, no. 1, pp. 12-16, 1990.
- [21] G. Wozniak, K. Wozniak and H. Bergelt, "On the influence of buoyancy on the surface tension driven flow around a bubble on a heated wall", *Experiments in Fluids*, vol. 21, no. 3, pp. 181-186, 1996.
- [22] Y. Kamotani, S. Ostrach and A. Pline, "Analysis of velocity data taken in Surface Tension Driven Convection Experiment in microgravity", *Physics of Fluids*, vol. 6, no. 11, p. 3601, 1994.
- [23] O. Ruiz and W. Black, "Evaporation of Water Droplets Placed on a Heated Horizontal Surface", *J. Heat Transfer*, vol. 124, no. 5, p. 854, 2002.
- [24] A. Kirdyashkin, "Thermogravitational and thermocapillary flows in a horizontal liquid layer under the conditions of a horizontal temperature gradient", *International Journal of Heat and Mass Transfer*, vol. 27, no. 8, pp. 1205-1218, 1984.
- [25] D. Villers and J. Platten, "Coupled buoyancy and Marangoni convection in acetone: experiments and comparison with numerical simulations", *J. Fluid Mech.*, vol. 234, no. -1, p. 487, 1992.
- [26] P. Lin, B. Fu and C. Pan, "Critical heat flux on flow boiling of methanol–water mixtures in a diverging microchannel with artificial cavities", *International Journal of Heat and Mass Transfer*, vol. 54, no. 15-16, pp. 3156-3166, 2011.
- [27] R. Savino and S. Fico, "Buoyancy and surface tension driven convection around a bubble", *Physics of Fluids*, vol. 18, no. 5, p. 057104, 2006.

[28] Nanayakkara et al., "The Effect of AC Frequency on the Electrowetting Behavior of Ionic Liquids", *Analytical Chemistry*, 2010, 82, pp.3146-3154.

[29] "Nikon MicroscopyU | Polarized Light Microscopy", *Microscopyu.com*, 2016. [Online]. Available: <http://www.microscopyu.com/articles/polarized/polarizedintro.html>.

[30] "TLC products for use and testing in research applications", LCR Hallcrest Research and Testing Products, <http://www.hallcrest.com/downloads/RT001%20R&T%20Prods%20Info%20Package.pdf>.

[31] D. Logan and D. Logan, *A first course in the finite element method*. Pacific Grove, CA: Brooks/Cole, 2002.

## BIOGRAPHICAL INFORMATION

Ajinkya Shrikrishna Shetye received his bachelor degree from University of Mumbai, India, in 2012. He joined The University of Texas at Arlington (UTA) in 2014. He is currently a member of Integrated Micro-Nano fluidic systems laboratory at UTA. His research interest lies in microfluidics, thermal management mems fabrication and interfacial phenomena.